

1 **Interruption of glucagon signaling augments islet non-alpha cell proliferation in SLC7A2-**  
2 **and mTOR-dependent manners**

3

4 Katie C. Coate<sup>1,2,6\*</sup>, Chunhua Dai<sup>1\*</sup>, Ajay Singh<sup>1</sup>, Jade Stanley<sup>2</sup>, Brittney A. Covington<sup>2</sup>, Amber  
5 Bradley<sup>1</sup>, Favour Oladipupo<sup>1</sup>, Yulong Gong<sup>2</sup>, Scott Wisniewski<sup>1</sup>, Erick Spears<sup>1</sup>, Greg  
6 Poffenberger<sup>1</sup>, Alexandria Bustabad<sup>1</sup>, Tyler Rodgers<sup>1</sup>, Nandita Dey<sup>1</sup>, Leonard D. Shultz<sup>3</sup>, Dale L.  
7 Greiner<sup>4</sup>, Hai Yan<sup>5</sup>, Alvin C. Powers<sup>1,2,6#</sup>, Wenbiao Chen<sup>2#</sup>, E. Danielle Dean<sup>1,2#</sup>

8

9 <sup>1</sup>Division of Diabetes, Endocrinology and Metabolism, Department of Medicine, Vanderbilt  
10 University Medical Center, Nashville, TN

11 <sup>2</sup>Department of Molecular Physiology and Biophysics, Vanderbilt University, Nashville, TN

12 <sup>3</sup>The Jackson Laboratory, Bar Harbor, ME

13 <sup>4</sup>Program in Molecular Medicine, Diabetes Center of Excellence, University of Massachusetts  
14 Chan Medical School, Worcester, MA

15 <sup>5</sup>REMD Biotherapeutics Inc., Camarillo, CA

16 <sup>6</sup>Department of Veterans Affairs, Tennessee Valley Healthcare System, Nashville, TN

17 \* equal contribution

18 # Corresponding authors: E. Danielle Dean, [danielle.dean@vumc.org](mailto:danielle.dean@vumc.org); Alvin C. Powers,  
19 [al.powers@vumc.org](mailto:al.powers@vumc.org); Wenbiao Chen, [wenbiao.chen@vanderbilt.edu](mailto:wenbiao.chen@vanderbilt.edu)

20

21

22

23

24

25

26

27 **ABSTRACT**

28 **Objective:** Dysregulated glucagon secretion and inadequate functional beta cell mass are  
29 hallmark features of diabetes. While glucagon receptor (GCGR) antagonism ameliorates  
30 hyperglycemia and elicits beta cell regeneration in pre-clinical models of diabetes, it also  
31 promotes alpha and delta cell hyperplasia. We sought to investigate the mechanism by which  
32 loss of glucagon action impacts pancreatic islet non-alpha cells, and the relevance of these  
33 observations in a human islet context.

34 **Methods:** We used zebrafish, rodents, and transplanted human islets comprising six different  
35 models of interrupted glucagon signaling to examine their impact on delta and beta cell  
36 proliferation and mass. We also used models with global deficiency of the cationic amino acid  
37 transporter, SLC7A2, and mTORC1 inhibition via rapamycin, to determine whether amino acid-  
38 dependent nutrient sensing was required for islet non-alpha cell growth.

39 **Results:** Inhibition of glucagon signaling stimulated delta cell proliferation in mouse and  
40 transplanted human islets, and in mouse islets. This was rapamycin-sensitive and required  
41 SLC7A2. Likewise, *gcgr* deficiency augmented beta cell proliferation via SLC7A2- and  
42 mTORC1-dependent mechanisms in zebrafish and promoted cell cycle engagement in rodent  
43 beta cells but was insufficient to drive a significant increase in beta cell mass in mice.

44 **Conclusion:** Our findings demonstrate that interruption of glucagon signaling augments islet  
45 non-alpha cell proliferation in zebrafish, rodents, and transplanted human islets in a manner  
46 requiring SLC7A2 and mTORC1 activation. An increase in delta cell mass may be leveraged for  
47 future beta cell regeneration therapies relying upon delta cell reprogramming.

48

49

50

51

52

## 53 1. INTRODUCTION

54 Diabetes is a multifactorial disease, but insufficient insulin secretion due to inadequate  
55 functional beta cell mass and dysregulated, often increased, glucagon secretion are  
56 fundamental to essentially all forms of diabetes and contribute to hyperglycemia.<sup>1-6</sup> The utility of  
57 glucagon receptor (GCGR) antagonism as a means of treating diabetic hyperglycemia has been  
58 intensively examined because it markedly improves glycemic control in diabetic rodents, non-  
59 human primates, and humans.<sup>7-10</sup> More recently, studies have shown that inducible elimination  
60 of glucagon action by administration of a GCGR monoclonal antibody (GCGR-Ab) enhances  
61 beta cell survival, regeneration, and function in pre-clinical models of type 1 (T1D) and type 2  
62 (T2D) diabetes.<sup>11-16</sup>

63  
64 However, inhibition of glucagon action elicits adverse effects as well, including increased serum  
65 and liver lipid levels, increased blood pressure, and robust pancreatic islet alpha cell  
66 hyperplasia.<sup>10</sup> We and others<sup>17-21</sup> have shown that the response of islet alpha cells to GCGR  
67 antagonism is caused by disruption of the liver-alpha cell axis, which results in  
68 hyperaminoacidemia, hyperglucagonemia, and rapamycin-sensitive alpha cell proliferation  
69 through a mechanism also involving induction of a glutamine transporter, *Slc38a5*, in alpha  
70 cells.<sup>19,20</sup> Recently, we extended these observations by showing that the alpha cell-enriched  
71 cationic amino acid transporter, *Slc7a2*, is required for high amino acid-stimulated mTOR  
72 activation, *Slc38a5* induction, alpha cell proliferation, and islet hormone secretion<sup>22</sup>,  
73 underscoring a prominent role for amino acids in the regulation of alpha cell function and  
74 phenotypes.<sup>23</sup>

75  
76 Interestingly, pancreatic islet non-alpha cells, namely delta and beta cells, have also been  
77 shown to be impacted by GCGR antagonism.<sup>17,24-26</sup> For example, constitutive ablation of the  
78 *Gcgr* gene was associated with 2- and 3-fold increases in pancreatic delta cell number and

79 somatostatin content, respectively, and increased postnatal beta cell proliferation and  
80 mass.<sup>17,24,25</sup> Furthermore, some<sup>11,26</sup> but not all<sup>18-20,27</sup> studies have shown that GCGR-Ab  
81 treatment increases pancreatic delta and beta cell numbers in mice and cynomolgus monkeys,  
82 respectively. However, the mechanism by which constitutive or inducible elimination of glucagon  
83 action elicits changes in islet non-alpha cells under insulin-sufficient conditions, and the  
84 relevance of these observations in a human islet context, are unknown.

85

86 Here, we used several complementary approaches to show that interruption of glucagon  
87 signaling augments islet non-alpha cell proliferation in SLC7A2- and mTORC1-dependent  
88 manners. We found that constitutive and inducible elimination of glucagon action stimulated  
89 delta cell proliferation and mass expansion in mouse and transplanted human islets, and that in  
90 mouse islets, this required mTORC1 activation and the amino acid transporter, SLC7A2.

91 Likewise, we found that *gcgr* deficiency increased beta cell number in a SLC7A2- and  
92 rapamycin-sensitive manner in zebrafish and promoted cell cycle engagement in rodent beta  
93 cells but was insufficient to drive a significant increase in beta cell mass in mice. Our findings  
94 highlight key differences in the regulation of beta versus delta and alpha cell proliferation and  
95 reveal a new mechanism linking inhibition of glucagon signaling to expansion of islet delta cell  
96 mass that may be leveraged for future beta cell regeneration therapies via delta cell  
97 reprogramming.<sup>28,29</sup>

98

99

100

## 101 2. MATERIALS AND METHODS

### 102 2.1. Mouse studies

103 All studies were performed at Vanderbilt University Medical Center and conducted in  
104 accordance with protocols and guidelines approved by the Vanderbilt University Institutional  
105 Animal Care and Use Committee. Mice were provided ad libitum access to standard rodent  
106 chow and water and housed under a 12-hour light/12-hour dark cycle. The following mice were  
107 obtained from The Jackson Laboratory: *Gcg*<sup>-/-</sup> (NOD.Cg-*Gcg*<sup>em1Dvs</sup> *Prkdc*<sup>scid</sup> *Il2rg*<sup>tm1Wjl</sup>/DvsJ,  
108 strain #: 029819)<sup>30</sup>, C57BL/6J (strain #000664), NSG (NOD.Cg-*Prkdc*<sup>scid</sup> *Il2rg*<sup>tm1Wjl</sup>/SzJ, strain #:  
109 005557)<sup>31</sup>, and *Slc7a2*<sup>-/-</sup> (B6.129S7-*Slc7a2*<sup>tm1Ctm</sup>/LellJ, strain #: 022767).<sup>32</sup> *Gcgr*<sup>-/-</sup> and *Gcgr*<sup>Hep-/-</sup>  
110 mice were generated as described previously.<sup>17</sup> Wildtype (+/+) and knockout (-/-) mice obtained  
111 from heterozygous crosses were used for all experiments. For inducible elimination of glucagon  
112 action, mice were treated once per week for up to 8 weeks with control (IgG or PBS) or 10mg/kg  
113 of a humanized monoclonal antibody (10mg/kg) targeting the glucagon receptor (GCGR-Ab;  
114 “Ab-4” and REMD 2.59)<sup>33</sup> via intraperitoneal (i.p.) injection.

115  
116 For transplantation experiments, mouse islets were isolated by intraductal infusion of  
117 collagenase P, separated via histopaque gradient, and cultured overnight in Roswell Park  
118 Memorial Institute complete medium (RPMI; 5.6 mmol/L glucose with 10% FBS) before  
119 transplantation. Islets were isolated from 13-15-week-old *Slc7a2*<sup>+/+</sup> and *Slc7a2*<sup>-/-</sup> mice and  
120 transplanted beneath the renal capsule of contralateral kidneys in 16-18-week-old syngeneic  
121 *Slc7a2*<sup>+/+</sup> recipients. Following 2 weeks of engraftment, *Slc7a2*<sup>+/+</sup> recipient mice were injected  
122 i.p. with control IgG or GCGR-Ab (10 mg/kg) once per week for 2 weeks, after which the kidneys  
123 were harvested for tissue embedding and graft analysis as described.<sup>22</sup> In the *Gcgr* mouse line,  
124 islets isolated from 14-week-old *Gcgr*<sup>+/+</sup> mice were transplanted beneath the renal capsule of  
125 14-week-old syngeneic *Gcgr*<sup>Flox</sup> or *Gcgr*<sup>Hep-/-</sup> recipients as described.<sup>17</sup> Human islet transplants  
126 were performed exactly as described.<sup>19</sup> Human islets were obtained from the Integrated Islet

127 Distribution Program (<https://iidp.coh.org/>) or the Human Pancreas Analysis Program  
128 (<https://hpap.pmacs.upenn.edu>).<sup>34,35</sup> Individual donor characteristics may be found in  
129 Supplemental Table 1 and Dean et al.<sup>19</sup>

130

## 131 **2.2. Zebrafish studies**

132 We used previously described *gcgra/b* double-knock<sup>19</sup> out (abbreviated *gcgr*<sup>-/-</sup> here) and *slc7a2*<sup>-/-</sup>  
133 zebrafish lines.<sup>22</sup> Proliferating beta cells were identified by incubating zebrafish embryos with 1  
134 mmol/l 5-ethynyl-2-deoxyuridine (EdU) at four days post-fertilization (dpf) and chasing them for  
135 24 hours. EdU was detected as described previously.<sup>36</sup> Beta cell number was measured by  
136 counting *Tg(ins:H2B-mcherry)* labeled beta cells in the islet of five dpf zebrafish as described.<sup>36</sup>  
137 In the rapamycin experiments, starting at 3 dpf zebrafish were treated with a concentration of  
138 200 nM rapamycin. Treatment continued for 3 days and then beta cell number was determined  
139 at 6 dpf in *gcgr*<sup>-/-</sup> and control fish.

140

## 141 **2.3. Immunofluorescence staining and image analysis**

142 Tissue preparation and sectioning were performed as described previously.<sup>19,22</sup> Tissue sections  
143 were stained for Ki67, a marker of cell proliferation (Abcam, ab15580), phosphorylated  
144 ribosomal protein S6 (pS6<sup>240/244</sup>), a marker of mTOR activation (Cell Signaling, #2215), and  
145 insulin (Dako, A0564), somatostatin (Santa Cruz, sc-7819), or glucagon (LSBio, LS-C202759) to  
146 mark beta, delta, and alpha cells, respectively. Alpha cells in *Gcg*<sup>-/-</sup> sections were identified by  
147 pro-glucagon staining (Cell Signaling, #8233). Whole pancreatic sections and islet grafts were  
148 imaged using a Scanscope FL System (Aperio Technologies) and an Olympus FV3000 laser  
149 scanning confocal microscope and analyzed using Halo image analysis software (Indica Labs).  
150 Colocalization of Ki67 with DAPI in insulin+ and somatostatin+ cells was determined by manual  
151 counting and a CytoNuclear FL v1.4 algorithm (Indica Labs). Percent beta and delta cell  
152 proliferation was quantified from at least 1500 beta and up to 1200 delta cells per animal (and at

153 least 450 beta and 400 delta cells per donor) by dividing the number of Ki67+/insulin+ or  
154 Ki67+/somatostatin+ cells by the total number of insulin+ or somatostatin+ cells, respectively.  
155 Beta and delta cell mass was determined using an area classifier in Halo and calculated as  
156 described.<sup>37</sup> Briefly, the fractional areas for insulin and somatostatin from 5-7 pancreatic  
157 sections of differing tissue depths were multiplied by the pancreas weight to obtain an estimate  
158 of total beta and delta cell mass.

159

#### 160 **2.4. Statistical Analyses**

161 All data are presented as mean  $\pm$  SEM. Comparisons between 2 groups were analyzed using  
162 unpaired two-tailed t tests. Comparisons between more than 2 groups were determined by one-  
163 way or two-way ANOVA with Fisher's LSD or Tukey's post-hoc tests.  $P < 0.05$  denotes  
164 statistical significance. Analyses were performed using Prism 9 software.

165

166

167

## 168 **3. RESULTS**

### 169 **3.1. Loss of glucagon action augments delta cell proliferation and mass expansion in**

170 **mouse and transplanted human islets.** To determine how interruption of glucagon signaling  
171 impacts pancreatic islet non-alpha cells, we first measured delta cell proliferation and mass in  
172 two different mouse models: one with constitutive global glucagon deficiency (*Gcg*<sup>-/-</sup>) and  
173 another with inducible elimination of glucagon action via treatment with a GCGR-Ab. We found  
174 that delta cell proliferation, quantified as the percentage of Ki67-positive delta cells, was  
175 increased by 4.7- and 6.2-fold in *Gcg*<sup>-/-</sup> and GCGR-Ab treated mice, respectively, compared with  
176 controls (**Fig 1A-C**). This resulted in a ~ 3-fold increase in delta cell mass compared to controls  
177 (**Fig 1D-F**). Consistent with earlier reports<sup>24,25</sup>, we also observed a distinctive shift in the  
178 distribution of somatostatin-positive cells from the mantle to the core of the islet in both *Gcg*<sup>-/-</sup>  
179 and GCGR-Ab treated mice (**Fig 1A and 1D**). To evaluate the translational relevance of these  
180 findings, we measured delta cell proliferation in human islets transplanted into  
181 immunocompromised recipient mice (i.e., NSG) treated with IgG (control) or GCGR-Ab and  
182 found a 3.5-fold increase in the percentage of Ki67-positive delta cells after 4 weeks of  
183 treatment (**Fig 1G-I**). Our findings suggest that interruption of glucagon signaling promotes islet  
184 delta cell mass expansion by stimulating delta cell proliferation in mouse and transplanted  
185 human islets.

186

### 187 **3.2. SLC7A2 and mTORC1 activation are required for delta cell proliferation in response** 188 **to interrupted glucagon signaling.** To gain insight into the mechanism(s) that may be driving

189 delta cell proliferation in *Gcg*<sup>-/-</sup> and GCGR-Ab treated mice, we first measured delta cell  
190 proliferation in mice with constitutive global inactivation of the cationic amino acid transporter,  
191 SLC7A2. We and others<sup>18-20</sup> have shown that GCGR-Ab-induced hyperaminoacidemia,  
192 especially arginine and glutamine, triggers pancreatic islet alpha cell proliferation in an mTOR-  
193 dependent manner, and that this response requires SLC7A2.<sup>22</sup> Here, we found that SLC7A2 is

194 also required, at least in part, for delta cell proliferation in response to GCGR-Ab treatment  
195 since the percentage of Ki67-positive delta cells was abrogated, albeit incompletely, in *Slc7a2*  
196 knockout (-/-) mice compared with wild-type (+/+) controls (**Fig 2A-B**). To delineate the  
197 intracellular signaling pathway involved, we immunostained for phosphorylated (p) S6 protein, a  
198 downstream target of mTOR kinase, and observed an 18-fold increase in the percentage of  
199 pS6-positive delta cells in islets of *Gcg*<sup>-/-</sup> compared with *Gcg*<sup>+/+</sup> mice, indicative of mTOR  
200 activation (**Fig 2C-D**). To determine whether mTOR signaling was required for delta cell  
201 proliferation, we co-treated mice with GCGR-Ab and rapamycin (RAPA), an mTOR inhibitor, and  
202 found that RAPA abolished GCGR-Ab-induced delta cell proliferation in C57BL6 mice (**Fig 2E-**  
203 **F**). These data indicate that loss of glucagon action stimulates RAPA-sensitive delta cell  
204 proliferation through a mechanism requiring, at least in part, the amino acid transporter  
205 SLC7A2.

206

### 207 **3.3. Loss of glucagon receptor function stimulates beta cell proliferation in a species-**

208 **specific manner.** Since the response of islet delta cells to interrupted glucagon signaling  
209 resembled that of alpha cells shown previously<sup>17-20,22,24,25,36,38</sup> we wanted to determine if this  
210 mechanism was likewise conserved in beta cells under insulin-sufficient conditions. First, we  
211 examined a zebrafish model with constitutive global deficiency of both forms of the *gcgr*<sup>36</sup>  
212 (*gcgra/b*<sup>-/-</sup>, abbreviated *gcgr*<sup>-/-</sup>) and found that beta cell proliferation and number were both  
213 increased in *gcgr*<sup>-/-</sup> zebrafish compared to WT (*gcgr*<sup>+/+</sup>) controls (**Fig 3A-B**). Furthermore, this  
214 response was significantly blunted in *slc7a2*<sup>-/-</sup>;*gcgr*<sup>-/-</sup> double mutants, or in *gcgr*<sup>-/-</sup> zebrafish  
215 treated with RAPA (**Fig 3C-D**). These data indicate that the mechanism for GCGR deficiency-  
216 induced delta and alpha cell mass expansion is conserved in zebrafish beta cells.

217 To examine the response of beta cells in a mammalian context, we treated adult  
218 C57BL6 mice with IgG or GCGR-Ab for 8 weeks and observed a 4.1-fold increase in the  
219 percentage of Ki67 positive beta cells (**Fig 3E-F**). This measure of beta cell proliferation was

220 also increased in mice with constitutive global inactivation of glucagon signaling (**Fig S1A-B**), as  
221 shown previously.<sup>25</sup> Furthermore, we detected an increase in beta cell proliferation in *Gcgr*<sup>+/+</sup>  
222 islets only when transplanted into liver-specific *Gcgr*<sup>-/-</sup> (*Gcgr*<sup>Hep<sup>-/-</sup>) and not *Gcgr*<sup>Flox</sup> mice (**Fig**  
223 **S1C-E**), supporting the premise that inhibition of hepatic glucagon action produces circulating  
224 factors that augment islet cell proliferation.<sup>15,18-20</sup></sup>

225 To determine whether the amino acid transporter SLC7A2 was required for beta cell  
226 proliferation, we treated *Slc7a2*<sup>+/+</sup> and *Slc7a2*<sup>-/-</sup> mice with IgG or GCGR-Ab for 2 weeks and  
227 found that the GCGR-Ab-induced increase in Ki67-positive beta cells (~2.8-fold) was abolished  
228 in *Slc7a2*<sup>-/-</sup> islets (**Fig 3G**), and in *Slc7a2*<sup>-/-</sup>, but not *Slc7a2*<sup>+/+</sup>, islets transplanted into *Slc7a2*<sup>+/+</sup>  
229 recipients (**Fig S2A-C**). These data suggest that SLC7A2 is required in an islet autonomous  
230 manner for GCGR-Ab-induced beta cell proliferation. In contrast to the response of mouse delta  
231 and zebrafish beta cells, however, we did not detect a coordinate increase in beta cell mass in  
232 GCGR-Ab-treated mice (**Fig S2D**). The discordance between beta cell proliferation and mass  
233 did not appear to be due to a detectable increase in beta cell death since we did not detect any  
234 TUNEL positive beta cells in islets of GCGR-Ab treated mice (data not shown). These findings  
235 imply that inducible elimination of glucagon action is sufficient to stimulate beta cell cycle entry,  
236 but insufficient to promote cell cycle completion in healthy mice.

237 Lastly, we sought to evaluate the translational relevance of these observations by  
238 measuring beta cell proliferation in transplanted human islets and likewise observed an increase  
239 in the mean percentage of Ki67-positive beta cells following 4 weeks of GCGR-Ab treatment  
240 (**Fig 3H-J**), though the magnitude of the response varied widely among donors and was lower  
241 than that of human delta cells.

242

243

244

#### 245 4. DISCUSSION

246 The mechanism linking inhibition of glucagon signaling to changes in pancreatic islet  
247 delta and beta cells, and the relevance of these observations in a human islet context, are  
248 unknown. In this study, we used zebrafish, rodents, and transplanted human islets comprising  
249 six different models of altered glucagon signaling to show that inhibition of glucagon action  
250 stimulated delta and beta cell proliferation via SLC7A2- and mTORC1-dependent mechanisms.  
251 Constitutive global deletion of *Gcg*, or inducible elimination of glucagon signaling with a GCGR-  
252 Ab, promoted RAPA-sensitive delta cell proliferation and mass expansion through a mechanism  
253 requiring the cationic amino acid transporter, SLC7A2. Likewise, we identified an increase in  
254 beta cell proliferation and mass in *gcgr*-deficient zebrafish that was abrogated upon deletion of  
255 SLC7A2 or treatment with RAPA. While constitutive and inducible inhibition of glucagon  
256 signaling also augmented the percentage of Ki67-positive beta cells in rodent islets, this  
257 resulted in only a modest, non-significant increase in beta cell mass. Consistent with previous  
258 reports in human alpha cells<sup>19,20</sup>, we also showed that GCGR-Ab treatment stimulated human  
259 delta, and to a lesser extent beta, cell proliferation in transplanted islets, highlighting the  
260 translational relevance of our observations.

261

262 We and others<sup>18-20</sup> showed previously that GCGR antagonism elicits  
263 hyperaminoacidemia, which promotes mTOR-dependent alpha cell hyperplasia through a  
264 mechanism involving induction of SLC38A5, a glutamine transporter, in alpha cells.<sup>19,20</sup> More  
265 recently, we found that SLC7A2, an arginine transporter, is the most highly expressed amino  
266 acid transporter in zebrafish, rodent, and human alpha cells and required for activation of  
267 mTORC1 signaling, induction of SLC38A5, and stimulation of alpha cell proliferation in response  
268 to GCGR antagonism.<sup>22</sup> Here, we extended these observations by demonstrating that SLC7A2  
269 and mTORC1 activation are likewise required for islet non-alpha cell proliferation in response to  
270 interrupted glucagon signaling. This was surprising since the expression of *Slc7a2* is much

271 lower in delta and beta cells compared to alpha cells.<sup>22</sup> Because we used mice with constitutive  
272 global deletion of SLC7A2, we cannot delineate the direct versus indirect requirement for this  
273 transporter on delta and/or beta cell proliferation. Notwithstanding, we showed that GCGR-Ab  
274 treatment augmented the percentage of Ki67-positive beta cells in transplanted donor islets  
275 from *Slc7a2*<sup>+/+</sup>, but not *Slc7a2*<sup>-/-</sup>, mice supporting at least an islet-autonomous role for this  
276 transporter in amino acid-regulated cell proliferation. However, the possibility cannot be  
277 excluded that GCGR antagonism-dependent proliferative signal(s) emanating from SLC7A2-  
278 enriched alpha cells act in a paracrine manner on neighboring delta and/or beta cells to promote  
279 their proliferation. Future studies using conditional *Slc7a2* gene targeting approaches in islet  
280 delta, beta, and/or alpha cells will be necessary to delineate its requirement in specific  
281 endocrine cell subsets.

282

283 We were also surprised to find that mTORC1 signaling was required for islet non-alpha  
284 cell proliferation, since previous studies reported GCGR-Ab-mediated activation of S6 protein, a  
285 downstream target of mTORC1, in only rare beta<sup>20</sup> or delta<sup>19</sup> cells, and the results are  
286 conflicting. Here, we observed an 18-fold increase in the percentage of pS6-positive delta cells  
287 in *Gcgr*<sup>-/-</sup> islets, indicative of heightened mTORC1 activity. It is possible that the pattern of S6  
288 activation in islet cells differs between models of constitutive versus inducible elimination of  
289 glucagon action. Nevertheless, we showed that pharmacologic inhibition of mTORC1 signaling  
290 with RAPA abolished delta cell proliferation in GCGR-Ab-treated mice, and beta cell proliferation  
291 in *gcgr* deficient zebrafish, supporting a central role for mTORC1-dependent nutrient sensing in  
292 islet non-alpha cell proliferation in non-diabetic models.

293

294 Our results agree with previous studies in *Gcgr*<sup>-/-</sup> mice, which showed up to 3.5-fold  
295 increases in islet delta cell number, mass, and pancreatic somatostatin content.<sup>24,25</sup> These  
296 studies also identified a shift in the labeling pattern of somatostatin-positive cells from being

297 restricted to the mantle zone in *Gcgr*<sup>+/+</sup> islets to being scattered within the core as well in *Gcgr*<sup>-/-</sup>  
298 islets, much like alpha cells.<sup>24,25</sup> We confirmed and extended these observations in *Gcgr*<sup>-/-</sup> mice  
299 by showing that the increase in delta cell mass was due, at least in part, to delta cell  
300 proliferation as evidenced by a 4.7-fold increase in the percentage of Ki67-positive delta cells.  
301 More recently, Gu et al.<sup>26</sup> showed that treatment of C57BL6 mice with a GCGR-Ab at a weekly  
302 dose of 5 mg/kg for 4 weeks increased islet delta cell number by ~35% in association with  
303 marginally significant (P=0.05) delta cell proliferation. Conversely, we showed that treatment of  
304 C57BL6 mice with a GCGR-Ab at a weekly dose of 10 mg/kg for 8 weeks triggered a 6.2-fold  
305 increase in delta cell proliferation and a 2.5-fold increase in delta cell mass. These  
306 discrepancies are likely explained by differences in the dose and/or duration of GCGR-Ab  
307 exposure, since Kim et al.<sup>20</sup> also found no change in pancreatic delta cell mass in C57BL6 mice  
308 after 3 weeks of GCGR-Ab treatment at a weekly dose of only 3 mg/kg.

309  
310 The impact of interrupted glucagon signaling on beta cell proliferation and mass  
311 expansion under insulin-sufficient conditions is inconclusive. Several studies<sup>18-20,27,30</sup>, primarily in  
312 rodent models of inducible elimination of glucagon action, have failed to detect an increase in  
313 beta cell proliferation or mass. On the other hand, constitutive global or liver-specific ablation of  
314 the *Gcgr* gene was associated with increased postnatal beta cell proliferation<sup>25</sup> and up to a 1.7-  
315 fold increase in beta cell mass.<sup>17,25</sup> Furthermore, Xi et al.<sup>11</sup> found a ~20% increase in the  
316 percentage of insulin-positive cells in islets of healthy cynomolgus monkeys treated with GCGR-  
317 Ab at a weekly dose of 60 mg/kg for 13 weeks, but it is unknown if this was due to an increase  
318 in beta cell proliferation. Here, we showed a significant increase in beta cell mass in *gcgr*-  
319 deficient zebrafish, but not in GCGR-Ab treated mice, despite cell cycle engagement as  
320 evidenced by 2- to 4-fold increases in the percentage of Ki67 positive beta cells. An uncoupling  
321 of beta cell cycle entry from cell cycle completion was also observed by Furth-Lavi and  
322 colleagues<sup>39</sup> in a diabetic rodent model of extreme beta cell-ablation, where some beta cells

323 were capable of entering the cell cycle but failed to complete it under conditions of severe, but  
324 not moderate, hyperglycemia. In pre-clinical models of T1D and T2D, however, GCGR  
325 antagonism improves glycemia and readily promotes the regeneration of functional beta cell  
326 mass through, for example, beta cell proliferation and alpha-to-beta-cell transdifferentiation.<sup>11-16</sup>  
327 These studies suggest that the blood glucose level and/or magnitude of insulin deficiency may  
328 be determinants of beta cell regenerative capacity, and by extension, beta cell mass expansion,  
329 in diabetic rodent models. We posit that under healthy, insulin-sufficient conditions, rodent beta  
330 cells, but not alpha or delta cells, require additional proliferative signals – or disinhibition of  
331 repressive signals – for GCGR antagonism to promote cell cycle completion and an increase in  
332 beta cell mass. Tight control over insulin production is necessary to protect against  
333 hypoglycemia and may reflect physiologic autoregulation of beta cell mass in healthy animals.  
334 Species-specific differences in the response of beta cells to GCGR loss likely reflect the  
335 heightened plasticity, regenerative capacity and developmental stages of zebrafish versus  
336 mammalian islet cells.<sup>40-43</sup> Future studies aimed at identifying the extra- and/or intra-cellular  
337 effectors that couple beta cell cycle engagement with cell cycle completion in health and  
338 diabetes will shed new light on unique mechanisms of mammalian beta cell regulation.

339

340         These studies demonstrate a physiologic role for glucagon in the regulation of islet delta  
341 and beta cell mass and expose notable differences in their proliferative capacity in healthy mice.  
342 Future studies should address how amino acid-dependent nutrient sensing stimulates islet non-  
343 alpha cell proliferation, and whether GCGR-Ab induces delta cell mass expansion in diabetic  
344 models. By enhancing our understanding of the mechanism(s) linking inhibition of glucagon  
345 action to expansion of islet cell mass, we may improve our ability to mitigate the negative side  
346 effects of GCGR antagonism while leveraging its favorable effects, including the possibility for  
347 beta cell regeneration therapies relying upon delta (and/or alpha) cell reprogramming in T1D  
348 and T2D.<sup>26,28,29</sup>

349

350

351 **DECLARATION OF COMPETING INTERESTS**

352 The authors declare no conflicts of interests.

353

354

355 **CRedit AUTHORSHIP CONTRIBUTION STATEMENT**

356 **Katie C. Coate:** Conceptualization, Formal analysis, Validation, Investigation, Visualization,

357 Supervision, Project Administration, Funding acquisition, Writing – original draft, Writing –

358 review and editing; **Chunhua Dai:** Conceptualization, Methodology, Formal analysis, Validation,

359 Investigation, Visualization, Supervision, Project Administration, Writing – review and editing;

360 **Ajay Singh:** Investigation, Validation, Formal analysis; **Jade Stanley:** Investigation, Validation,

361 Formal analysis; **Brittney A. Covington:** Investigation, Validation, Formal analysis; **Amber**

362 **Bradley:** Software, Investigation, Validation; **Favour Oladipupo:** Investigation, Validation,

363 Formal analysis; **Yulong Gong:** Investigation, Validation, Formal analysis; **Scott Wisniewski:**

364 Investigation, Validation, Formal analysis; **Erick Spears:** Resources, Methodology,

365 Investigation; **Greg Poffengerber:** Methodology; **Alexandra Bustabad:** Investigation,

366 Validation, Formal analysis; **Tyler Rodgers:** Investigation, Validation, Formal analysis; **Nandita**

367 **Dey:** Investigation, Validation; **Leonard D. Shultz:** Resources, Writing – review and editing;

368 **Dale L. Greiner:** Resources, Writing – review and editing; **Hai Yan:** Resources; **Alvin C.**

369 **Powers:** Conceptualization, Resources, Writing – review and editing, Supervision, Project

370 administration, Funding Acquisition; **Wenbiao Chen:** Conceptualization, Resources, Writing –

371 review and editing, Supervision, Project administration, Funding Acquisition; **E. Danielle Dean:**

372 Conceptualization, Methodology, Validation, Investigation, Formal Analysis, Visualization,

373 Resources, Writing – review and editing, Supervision, Project administration, Funding

374 Acquisition

375

376 **ACKNOWLEDGEMENTS**

377 This research was performed using resources and/or funding provided by the following: JDRF

378 SRA-149-Q-R (to A.C.P. and E.D.D.), R01DK117147 (to W.C. and A.C.P.), an administrative

379 supplement to R01DK117147 (to K.C.C.), R01DK132669 (to E.D.D.), K01DK117969 (to

380 E.D.D.), the Human Islet Research Network (UC4 DK104211 and DK112232), R24DK106755

381 (to A.C.P.), DK104218 and OD0426640 (to D.L.G and L.D.S.), P30DK020593 (Vanderbilt

382 Diabetes Research and Training Center), P30DK058404 (Vanderbilt University Medical Center's

383 Digestive Diseases Research Center), T35DK007383 (Vanderbilt Student Research Training

384 Program), and the Department of Veterans Affairs (BX000666 to A.C.P.). Islet isolation and

385 slide scanning was performed using the Islet and Pancreas Analysis (IPA) Core supported by

386 the Vanderbilt Diabetes Research Center (NIH grant P30DK020593).

387

388

389

390

391

## 392 REFERENCES

- 393 1. Muller WA, Faloona GR, Aguilar-Parada E, Unger RH. Abnormal alpha-cell function in  
394 diabetes. Response to carbohydrate and protein ingestion. *N Engl J Med*.  
395 1970;283(3):109-115.
- 396 2. Unger R, Orci L. THE ESSENTIAL ROLE OF GLUCAGON IN THE PATHOGENESIS  
397 OF DIABETES MELLITUS. *The Lancet*. 1975;305(7897):14-16.
- 398 3. Kahn SE. The Importance of  $\beta$ -Cell Failure in the Development and Progression of Type  
399 2 Diabetes. *The Journal of Clinical Endocrinology & Metabolism*. 2001;86(9):4047-4058.
- 400 4. Dunning BE, Gerich JE. The role of alpha-cell dysregulation in fasting and postprandial  
401 hyperglycemia in type 2 diabetes and therapeutic implications. *Endocr Rev*.  
402 2007;28(3):253-283.
- 403 5. Hudish LI, Reusch JEB, Sussel L.  $\beta$  Cell dysfunction during progression of metabolic  
404 syndrome to type 2 diabetes. *The Journal of Clinical Investigation*. 2019;129(10):4001-  
405 4008.
- 406 6. Oram RA, Sims EK, Evans-Molina C. Beta cells in type 1 diabetes: mass and function;  
407 sleeping or dead? *Diabetologia*. 2019;62(4):567-577.
- 408 7. Miyama K, Elbarbry F, Bzowycykj A. Glucagon receptor antagonists for diabetes mellitus  
409 treatment: A systematic literature review. *The FASEB Journal*. 2019;33(S1):514.515-  
410 514.515.
- 411 8. Jia Y, Liu Y, Feng L, Sun S, Sun G. Role of Glucagon and Its Receptor in the  
412 Pathogenesis of Diabetes. *Front Endocrinol (Lausanne)*. 2022;13:928016.
- 413 9. Pettus J, Boeder SC, Christiansen MP, et al. Glucagon receptor antagonist volagidemab  
414 in type 1 diabetes: a 12-week, randomized, double-blind, phase 2 trial. *Nat Med*.  
415 2022;28(10):2092-2099.
- 416 10. Haedersdal S, Andersen A, Knop FK, Vilsboll T. Revisiting the role of glucagon in health,  
417 diabetes mellitus and other metabolic diseases. *Nat Rev Endocrinol*. 2023.
- 418 11. Xi Y, Song B, Ngan I, et al. Glucagon-receptor-antagonism-mediated beta-cell  
419 regeneration as an effective anti-diabetic therapy. *Cell Rep*. 2022;39(9):110872.
- 420 12. Wei T, Cui X, Jiang Y, et al. Glucagon Acting at the GLP-1 Receptor Contributes to beta-  
421 Cell Regeneration Induced by Glucagon Receptor Antagonism in Diabetic Mice.  
422 *Diabetes*. 2023.
- 423 13. Wei R, Gu L, Yang J, et al. Antagonistic Glucagon Receptor Antibody Promotes alpha-  
424 Cell Proliferation and Increases beta-Cell Mass in Diabetic Mice. *iScience*. 2019;16:326-  
425 339.
- 426 14. Wang MY, Dean ED, Quittner-Strom E, et al. Glucagon blockade restores functional  
427 beta-cell mass in type 1 diabetic mice and enhances function of human islets. *Proc Natl*  
428 *Acad Sci U S A*. 2021;118(9).
- 429 15. Cui X, Feng J, Wei T, et al. Pancreatic alpha cell glucagon-liver FGF21 axis regulates  
430 beta cell regeneration in a mouse model of type 2 diabetes. *Diabetologia*.  
431 2023;66(3):535-550.
- 432 16. Cui X, Feng J, Wei T, et al. Pro-alpha-cell-derived beta-cells contribute to beta-cell  
433 neogenesis induced by antagonistic glucagon receptor antibody in type 2 diabetic mice.  
434 *iScience*. 2022;25(7):104567.
- 435 17. Longuet C, Robledo AM, Dean ED, et al. Liver-specific disruption of the murine glucagon  
436 receptor produces alpha-cell hyperplasia: evidence for a circulating alpha-cell growth  
437 factor. *Diabetes*. 2013;62(4):1196-1205.
- 438 18. Solloway MJ, Madjidi A, Gu C, et al. Glucagon Couples Hepatic Amino Acid Catabolism  
439 to mTOR-Dependent Regulation of alpha-Cell Mass. *Cell Rep*. 2015;12(3):495-510.

- 440 19. Dean ED, Li M, Prasad N, et al. Interrupted Glucagon Signaling Reveals Hepatic alpha  
441 Cell Axis and Role for L-Glutamine in alpha Cell Proliferation. *Cell Metab.*  
442 2017;25(6):1362-1373 e1365.
- 443 20. Kim J, Okamoto H, Huang Z, et al. Amino Acid Transporter Slc38a5 Controls Glucagon  
444 Receptor Inhibition-Induced Pancreatic alpha Cell Hyperplasia in Mice. *Cell Metab.*  
445 2017;25(6):1348-1361 e1348.
- 446 21. Richter MM, Galsgaard KD, Elmelund E, et al. The Liver- $\alpha$ -Cell Axis in Health and in  
447 Disease. *Diabetes.* 2022;71(9):1852-1861.
- 448 22. Spears E, Stanley JE, Shou M, et al. Pancreatic islet  $\alpha$  cell function and proliferation  
449 requires the arginine transporter SLC7A2. *bioRxiv.* 2023:2023.2008.2010.552656.
- 450 23. Dean ED. A Primary Role for  $\alpha$ -Cells as Amino Acid Sensors. *Diabetes.* 2020;69(4):542-  
451 549.
- 452 24. Gelling RW, Du XQ, Dichmann DS, et al. Lower blood glucose, hyperglucagonemia, and  
453 pancreatic alpha cell hyperplasia in glucagon receptor knockout mice. *Proc Natl Acad*  
454 *Sci U S A.* 2003;100(3):1438-1443.
- 455 25. Vuguin PM, Kedes MH, Cui L, et al. Ablation of the glucagon receptor gene increases  
456 fetal lethality and produces alterations in islet development and maturation.  
457 *Endocrinology.* 2006;147(9):3995-4006.
- 458 26. Gu L, Cui X, Lang S, Wang H, Hong T, Wei R. Glucagon receptor antagonism increases  
459 mouse pancreatic  $\delta$ -cell mass through cell proliferation and duct-derived neogenesis.  
460 *Biochemical and Biophysical Research Communications.* 2019;512(4):864-870.
- 461 27. Okamoto H, Kim J, Aglione J, et al. Glucagon Receptor Blockade With a Human  
462 Antibody Normalizes Blood Glucose in Diabetic Mice and Monkeys. *Endocrinology.*  
463 2015;156(8):2781-2794.
- 464 28. Carril Pardo CA, Massoz L, Dupont MA, et al. A  $\delta$ -cell subpopulation with a pro- $\beta$ -cell  
465 identity contributes to efficient age-independent recovery in a zebrafish model of  
466 diabetes. *eLife.* 2022;11:e67576.
- 467 29. Chera S, Baronnier D, Ghila L, et al. Diabetes recovery by age-dependent conversion of  
468 pancreatic delta-cells into insulin producers. *Nature.* 2014;514(7523):503-507.
- 469 30. Tellez K, Hang Y, Gu X, Chang CA, Stein RW, Kim SK. In vivo studies of glucagon  
470 secretion by human islets transplanted in mice. *Nat Metab.* 2020;2(6):547-557.
- 471 31. Shultz LD, Lyons BL, Burzenski LM, et al. Human lymphoid and myeloid cell  
472 development in NOD/LtSz-scid IL2R gamma null mice engrafted with mobilized human  
473 hemopoietic stem cells. *J Immunol.* 2005;174(10):6477-6489.
- 474 32. Nicholson B, Manner CK, Kleeman J, MacLeod CL. Sustained nitric oxide production in  
475 macrophages requires the arginine transporter CAT2. *J Biol Chem.* 2001;276(19):15881-  
476 15885.
- 477 33. Yan H, Gu W, Yang J, et al. Fully human monoclonal antibodies antagonizing the  
478 glucagon receptor improve glucose homeostasis in mice and monkeys. *J Pharmacol Exp*  
479 *Ther.* 2009;329(1):102-111.
- 480 34. Kaestner KH, Powers AC, Najj A, Atkinson MA. NIH Initiative to Improve Understanding  
481 of the Pancreas, Islet, and Autoimmunity in Type 1 Diabetes: The Human Pancreas  
482 Analysis Program (HPAP). *Diabetes.* 2019;68(7):1394-1402.
- 483 35. Shapira SN, Najj A, Atkinson MA, Powers AC, Kaestner KH. Understanding islet  
484 dysfunction in type 2 diabetes through multidimensional pancreatic phenotyping: The  
485 Human Pancreas Analysis Program. *Cell Metab.* 2022;34(12):1906-1913.
- 486 36. Li M, Dean ED, Zhao L, Nicholson WE, Powers AC, Chen W. Glucagon receptor  
487 inactivation leads to alpha-cell hyperplasia in zebrafish. *J Endocrinol.* 2015;227(2):93-  
488 103.
- 489 37. Golson ML, Bush WS, Brissova M. Automated quantification of pancreatic beta-cell  
490 mass. *Am J Physiol Endocrinol Metab.* 2014;306(12):E1460-1467.

- 491 38. Gu W, Yan H, Winters KA, et al. Long-term inhibition of the glucagon receptor with a  
492 monoclonal antibody in mice causes sustained improvement in glycemic control, with  
493 reversible alpha-cell hyperplasia and hyperglucagonemia. *J Pharmacol Exp Ther.*  
494 2009;331(3):871-881.
- 495 39. Furth-Lavi J, Hija A, Tornovsky-Babeay S, et al. Glycemic control releases regenerative  
496 potential of pancreatic beta cells blocked by severe hyperglycemia. *Cell Rep.*  
497 2022;41(9):111719.
- 498 40. Ye L, Robertson MA, Hesselson D, Stainier DY, Anderson RM. Glucagon is essential for  
499 alpha cell transdifferentiation and beta cell neogenesis. *Development.*  
500 2015;142(8):1407-1417.
- 501 41. Ninov N, Hesselson D, Gut P, Zhou A, Fidelin K, Stainier DY. Metabolic regulation of  
502 cellular plasticity in the pancreas. *Curr Biol.* 2013;23(13):1242-1250.
- 503 42. Ghaye AP, Bergemann D, Tarifeño-Saldivia E, et al. Progenitor potential of nkx6.1-  
504 expressing cells throughout zebrafish life and during beta cell regeneration. *BMC Biol.*  
505 2015;13:70.
- 506 43. Curado S, Anderson RM, Jungblut B, Mumm J, Schroeter E, Stainier DY. Conditional  
507 targeted cell ablation in zebrafish: a new tool for regeneration studies. *Dev Dyn.*  
508 2007;236(4):1025-1035.
- 509

510

511

512

513

514

515

516

517

518

519

520

521

522

523

524

525

526 **FIGURE LEGENDS**

527 Figure 1. **Loss of glucagon action augments delta cell proliferation and mass expansion**  
528 **in mouse and transplanted human islets.** (A) Representative images of pancreatic islet and  
529 delta cell proliferation in  $Gcg^{+/+}/Gcg^{-/-}$  (upper row) and IgG/GCGR-Ab-treated C57BL6 (bottom  
530 row) mice. Somatostatin (green), Ki67 (red), and DAPI (blue) are shown. White arrows indicate  
531 Ki67+ somatostatin+ cells. (B-C) Quantification of pancreatic islet delta cell proliferation in (B)  
532  $Gcg^{+/+}$  (black bar) and  $Gcg^{-/-}$  (red bar) mice (n=1-2 females and 2-3 males per genotype) and (C)  
533 control IgG (black bar) and GCGR-Ab-treated (blue bar) mice (all males, unpaired t test, \*\*\*p <  
534 0.001 versus  $Gcg^{+/+}$ , \*\*p < 0.01 versus IgG). (D) Representative images of pancreatic islet  
535 hormones in  $Gcg^{+/+}/Gcg^{-/-}$  (upper row) and IgG/GCGR-Ab-treated (bottom row) mice. Insulin  
536 (green), somatostatin (red), and pro-glucagon ( $Gcg^{+/+}/Gcg^{-/-}$ ; blue) or glucagon (IgG/GCGR-Ab;  
537 blue) are shown. (E-F) Pancreatic islet delta cell mass in (E)  $Gcg^{+/+}$  (black bar) and  $Gcg^{-/-}$  (red  
538 bar) mice (n=1-2 females and 3 males per genotype) and (F) control IgG (black bar) and GCGR-  
539 Ab-treated (blue bar) mice (all males, unpaired t test, \*\*p < 0.01 versus  $Gcg^{+/+}$  or IgG). (G)  
540 Schematic of approach for human islet subcapsular renal transplantation in NSG recipient mice  
541 followed by control IgG or GCGR-Ab treatment. Created with BioRender.com (H)  
542 Representative images of delta cell proliferation in human islet grafts after 4 weeks of control  
543 IgG (upper row) or GCGR-Ab-treatment (bottom row). Grafts were immunostained for  
544 somatostatin (green), Ki67 (red), and DAPI (blue). White dashed boxes indicate regions  
545 selected for insets. (I) Quantification of delta cell proliferation in transplanted human islets in  
546 control IgG (black circles) and GCGR-Ab-treated (orange circles) mice (n=3 donors [see  
547 Supplemental Table 1], unpaired t test, \*\*p < 0.01 versus IgG).

548

549 Figure 2. **SLC7A2 and mTOR activation are required for delta cell proliferation in response**  
550 **to interrupted glucagon signaling.** (A) Representative images of pancreatic islet delta cell  
551 proliferation in  $Slc7a2^{+/+}$  (upper row) and  $Slc7a2^{-/-}$  (bottom row) IgG/GCGR-Ab-treated mice.

552 Somatostatin (green), Ki67 (red), and DAPI (blue) are shown. White arrows indicate Ki67+  
553 somatostatin+ cells. **(B)** Quantification of pancreatic islet delta cell proliferation in *Slc7a2*<sup>+/+</sup>  
554 (black bars) and *Slc7a2*<sup>-/-</sup> (blue bars) IgG or GCGR-Ab-treated mice (n=4 females and 1-3  
555 males per genotype, one-way ANOVA with Tukey's multiple comparisons test, \*\*\*\*p < 0.0001  
556 versus *Slc7a2*<sup>+/+</sup> IgG, \*\*\*p < 0.001 versus *Slc7a2*<sup>+/+</sup> GCGR-Ab). **(C)** Representative images of  
557 pancreatic islets in *Gcg*<sup>+/+</sup>/*Gcg*<sup>-/-</sup> mice immunostained for somatostatin (green), phosphorylated  
558 ribosomal protein S6 (pS6<sup>240/244</sup>, red), and DAPI (blue). White arrows indicate pS6+  
559 somatostatin+ cells. White dashed boxes indicate regions selected for insets. **(D)** Quantification  
560 of the percentage of pS6+ somatostatin+ cells in *Gcg*<sup>+/+</sup> (black bar) and *Gcg*<sup>-/-</sup> (red bar)  
561 pancreatic islets (n=1-2 females and 3-4 males per genotype, unpaired t test, \*\*\*\*p < 0.0001  
562 versus *Gcg*<sup>+/+</sup>). **(E)** Schematic of approach for IgG/GCGR-Ab (once weekly) and rapamycin  
563 (RAPA; once daily) co-treatment in C57BL6 mice. Created with BioRender.com **(F)**  
564 Quantification of pancreatic islet delta cell proliferation in mice co-treated with IgG (black bars)  
565 or GCGR-Ab (blue and white bar) and PBS or RAPA (all males, one-way ANOVA with Tukey's  
566 multiple comparisons test, \*\*\*\*p < 0.0001 versus IgG, \*\*\*p < 0.001 versus PBS/GCGR-Ab).

567

568 **Figure 3. Loss of glucagon receptor function stimulates beta cell proliferation in a**  
569 **species-specific manner.** **(A)** Beta cells stained for EdU to assess their proliferation in 5 dpf  
570 (days post-fertilization) wild-type (*gcgr*<sup>+/+</sup>, black bar) and *gcgra/b*<sup>-/-</sup> (abbreviated *gcgr*<sup>-/-</sup>, green  
571 bar) zebrafish (n=8 per group, unpaired t test, \*\*p < 0.01 versus *gcgr*<sup>+/+</sup>). **(B)** Beta cell number in  
572 5 dpf *gcgr*<sup>+/+</sup> (black bar) and *gcgr*<sup>-/-</sup> (green bar) zebrafish (n=24-30 per group, unpaired t test,  
573 \*\*\*\*p < 0.0001 versus *gcgr*<sup>+/+</sup>). **(C)** Beta cell number after knockdown of *slc7a2* (+/+, black bar; -  
574 /-, green bar) in 5 dpf *gcgr*<sup>-/-</sup> zebrafish (n=8-15 per group, unpaired t test, \*\*\*\*p < 0.0001 versus  
575 *slc7a2*<sup>+/+</sup>). **(D)** Beta cell number in 6 dpf *gcgr*<sup>+/+</sup> (black bar) and *gcgr*<sup>-/-</sup> (green bar) zebrafish after  
576 3 days of treatment with PBS or RAPA (n=6-7 per group, one-way ANOVA with Fisher's LSD,  
577 \*\*\*\*p < 0.0001 versus PBS/*gcgr*<sup>+/+</sup>, \* p < 0.05 versus PBS/*gcgr*<sup>-/-</sup>). **(E)** Representative images of

578 pancreatic islet beta cell proliferation in IgG/GCGR-Ab-treated C57BL6 mice. Insulin (green),  
579 Ki67 (red), and DAPI (blue) are shown. White arrow indicates a Ki67+ insulin+ cell. (F)  
580 Quantification of pancreatic islet beta cell proliferation in control IgG (black bar) and GCGR-Ab-  
581 treated (blue bar) mice (all males, unpaired t test, \*\*p < 0.01 versus IgG). (G) Quantification of  
582 pancreatic islet beta cell proliferation in *Slc7a2*<sup>+/+</sup> (black bars) and *Slc7a2*<sup>-/-</sup> (blue bars) IgG or  
583 GCGR-Ab-treated mice (n=2-5 females and 3-6 males per group, one way ANOVA with Tukey's  
584 multiple comparisons test, \*\*p < 0.0001 versus *Slc7a2*<sup>+/+</sup> IgG, \*\*\*p < 0.001 versus *Slc7a2*<sup>+/+</sup>  
585 GCGR-Ab). (H) Schematic of approach for human islet subcapsular renal transplantation in  
586 NSG recipient mice followed by PBS or GCGR-Ab treatment. Created with BioRender.com (I)  
587 Representative images of beta cell proliferation in human islet grafts after 4 weeks of PBS or  
588 GCGR-Ab-treatment. Grafts were immunostained for insulin (green), Ki67 (red), and DAPI  
589 (blue). Dashed yellow lines indicate kidney-graft boundary. (J) Quantification of beta cell  
590 proliferation in transplanted human islets in PBS (black circles) or GCGR-Ab-treated (orange  
591 circles) mice (n=2 female and 5 male donors [see Supplemental Table 1], unpaired t test, \*p <  
592 0.05 versus PBS).

593

594 Supplemental Figure 1. **Genetic interruption of glucagon signaling stimulates beta cell**  
595 **proliferation in pancreatic and transplanted mouse islets.** (A-B) Quantification of pancreatic  
596 islet beta cell proliferation in (A) 6 week-old *Gcgr*<sup>+/+</sup> (black bar, all males) and *Gcgr*<sup>-/-</sup> (red striped  
597 bar, all males) and (B) 8 week-old *Gcgr*<sup>+/+</sup> (black bar) and *Gcgr*<sup>-/-</sup> (red bar) mice (n=2-4 females  
598 and 3 males per group, unpaired t test, \*\*\*p < 0.001 versus *Gcgr*<sup>+/+</sup>, \*p < 0.05 versus *Gcgr*<sup>+/+</sup>). (C)  
599 Schematic of approach for subcapsular renal transplantation of *Gcgr*<sup>+/+</sup> (wild type, WT) donor  
600 islets into control (*Gcgr*<sup>Flox</sup>) or liver-specific *Gcgr* knockout (*Gcgr*<sup>Hep-/-</sup>) recipient mice. Created  
601 with BioRender.com (D) Representative images of islet grafts from WT to Flox and WT to Hep<sup>-/-</sup>  
602 recipients after four weeks. Grafts are immunostained for insulin (green), Ki67 (red) and DAPI  
603 (blue). White arrows indicate Ki67+ insulin+ cells. Dashed yellow lines indicate kidney-graft

604 boundary. **(E)** Quantification of beta cell proliferation in transplanted islets from WT to Flox  
605 (black bar) and WT to Hep<sup>-/-</sup> (red striped bar) groups (n=4 males per group, unpaired t test, \*\*p <  
606 0.05 versus WT to Flox).

607

608 Supplemental Figure 2. SLC7A2-**dependent stimulated beta cell proliferation is islet**

609 **autonomous.** **(A)** Schematic of approach for subcapsular renal transplantation of *Slc7a2*<sup>+/+</sup>

610 (wild type, WT) and *Slc7a2*<sup>-/-</sup> (KO) donor islets into *Slc7a2*<sup>+/+</sup> (WT) recipient mice followed by

611 control IgG or GCGR-Ab treatment. Created with BioRender.com **(B)** Representative images of

612 *Slc7a2*<sup>+/+</sup> (upper row) and *Slc7a2*<sup>-/-</sup> (bottom row) islet grafts from *Slc7a2*<sup>+/+</sup> kidney capsules after

613 two weeks of IgG or GCGR-Ab treatment. Grafts are immunostained for insulin (green), Ki67

614 (red) and DAPI (blue). White arrows indicate Ki67+ insulin+ cells. Dashed yellow lines indicate

615 kidney-graft boundary. **(C)** Quantification of beta cell proliferation in transplanted islets from

616 *Slc7a2*<sup>+/+</sup> and *Slc7a2*<sup>-/-</sup> donors treated with IgG (black circles) or GCGR-Ab (blue circles; n=2

617 females and 2 males per treatment group, two-way ANOVA with Fisher's LSD test, \*\*p < 0.01

618 versus IgG treated). **(D)** Quantification of pancreatic islet beta cell mass in *Slc7a2*<sup>+/+</sup> (black bars)

619 and *Slc7a2*<sup>-/-</sup> (blue bars) IgG or GCGR-Ab-treated mice (n=2-5 females and 3-6 males per

620 group).

621

622

623

624

625

626

627

628

629

630

631

632 Supplemental Table 1: *Human Islet Donor Information.*  
633

Donor ID	Age	Ethnicity/Race	Sex	BMI (kg/m <sup>2</sup> )	HbA1c (%)	Cause of Death	Islet Source
AELC213	10	Hispanic/Latino	F	25.4	N/A	Head Trauma/Blunt Injury	Other
AFEA331	45	Black	M	29.3	5.0	CVA/ stroke	IIDP
AIFV371	28	Hispanic/Latino	F	24.7	5.0	CVA/ stroke	HPAP
1	32	N/A	M	29.5	N/A	N/A	IIDP
2	47	N/A	M	22.3	N/A	N/A	IIDP
3	55	N/A	M	28.4	N/A	N/A	IIDP
4	43	N/A	M	29.6	N/A	N/A	IIDP
5	46	N/A	M	28.8	N/A	N/A	IIDP
6	41	N/A	F	31.1	N/A	N/A	IIDP
7	47	N/A	F	25.6	N/A	N/A	IIDP
8	52	N/A	M	33.2	N/A	N/A	IIDP

634  
635  
636  
637  
638

**Figure 1**

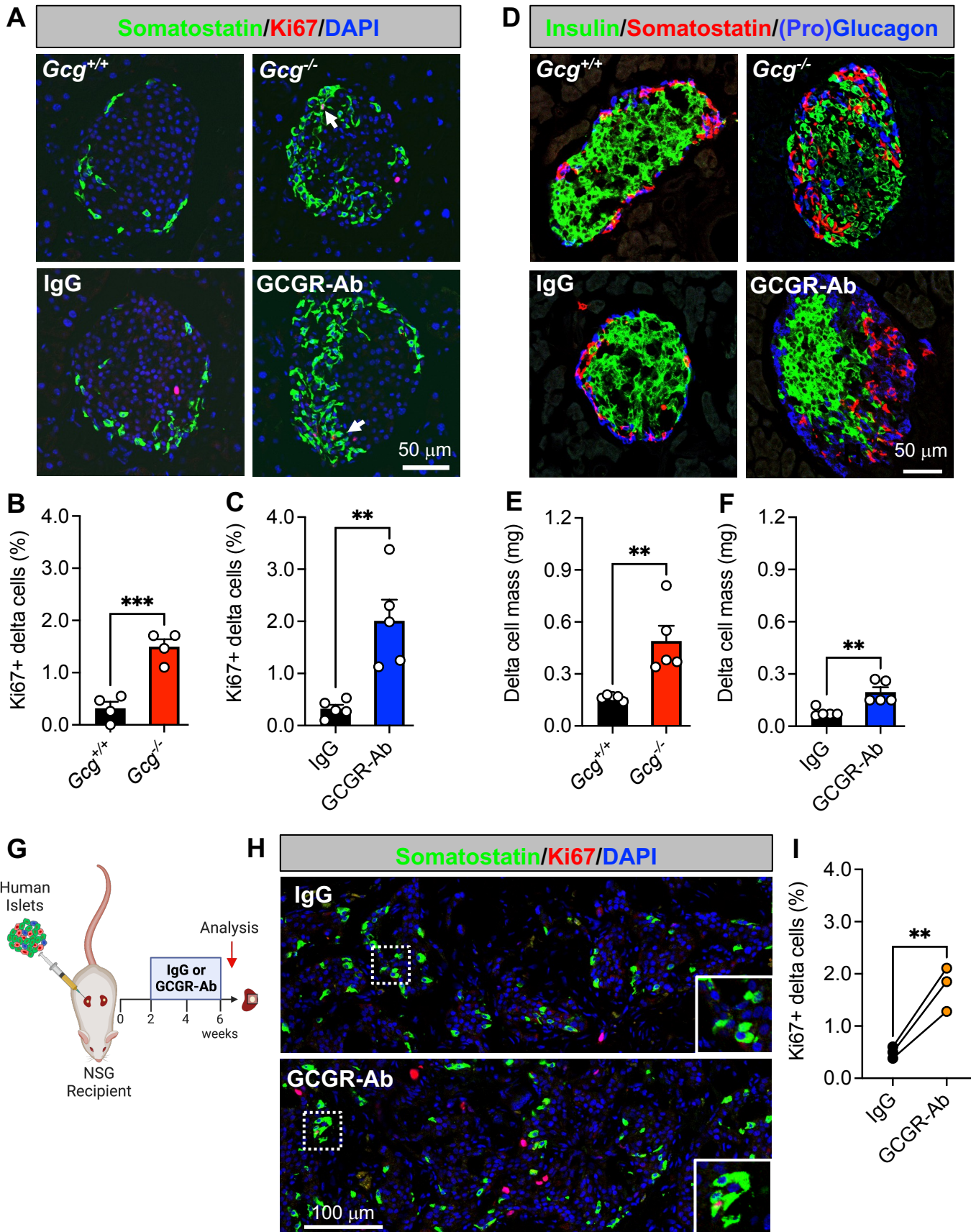


**Figure 2**

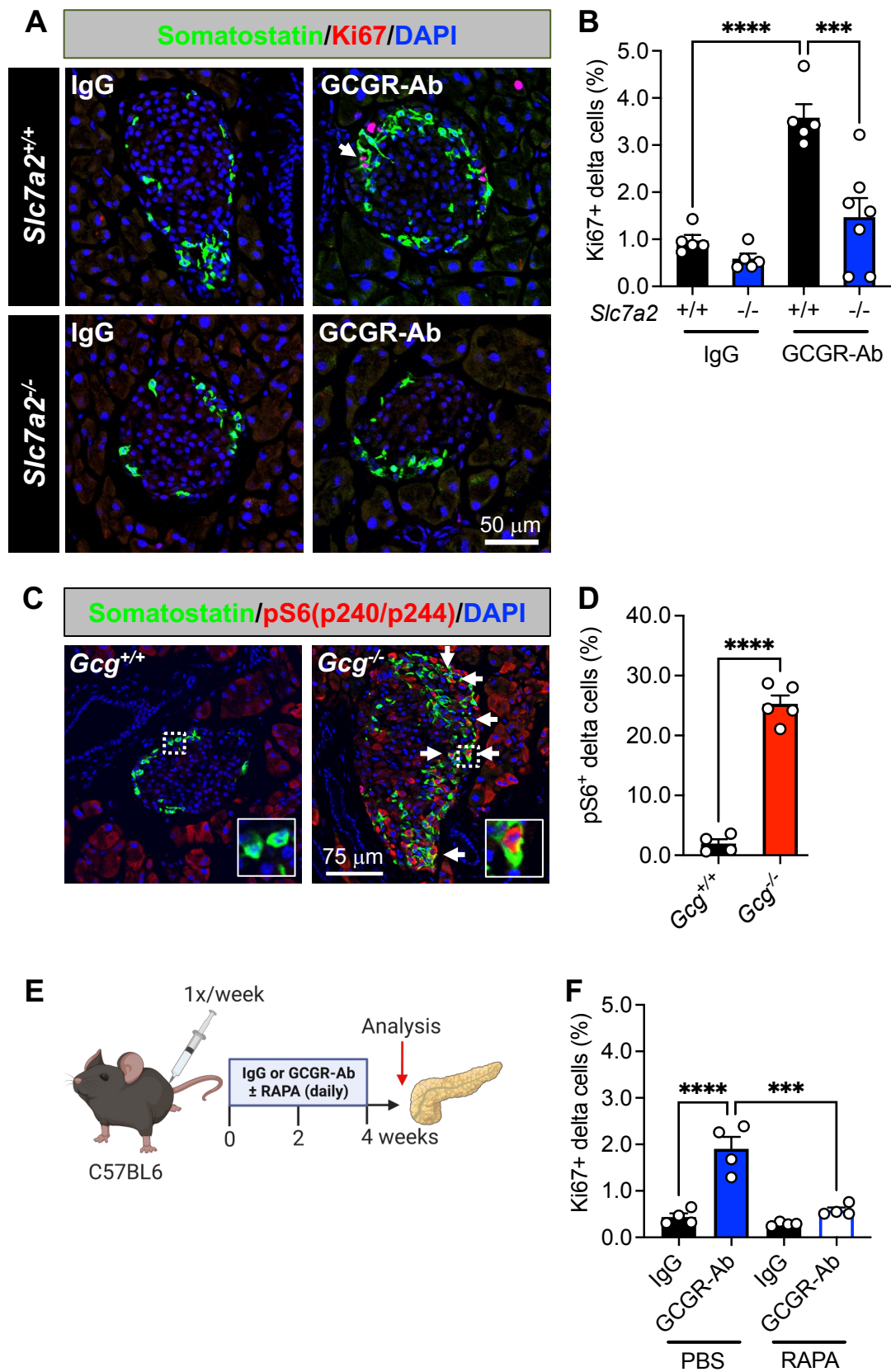
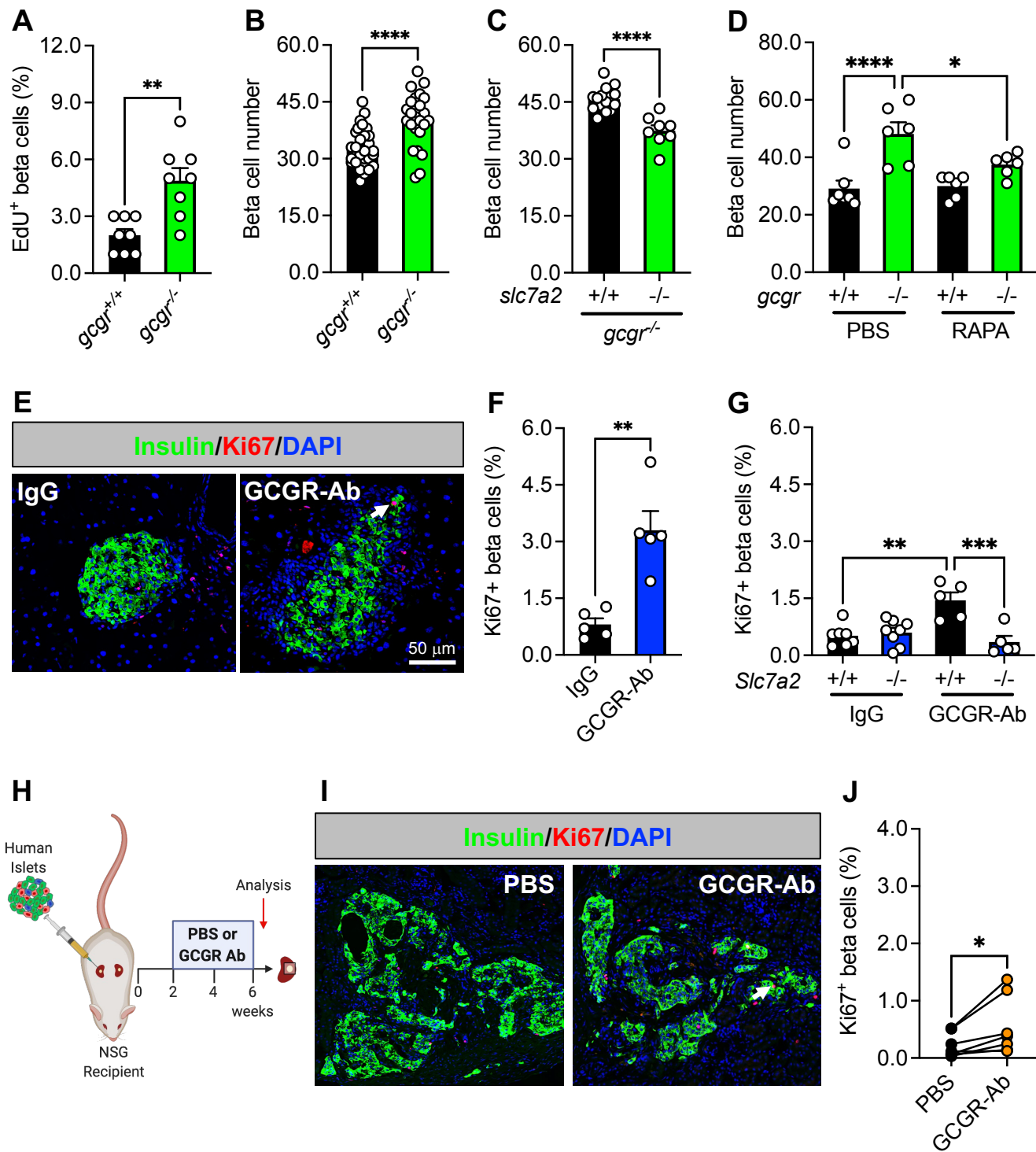
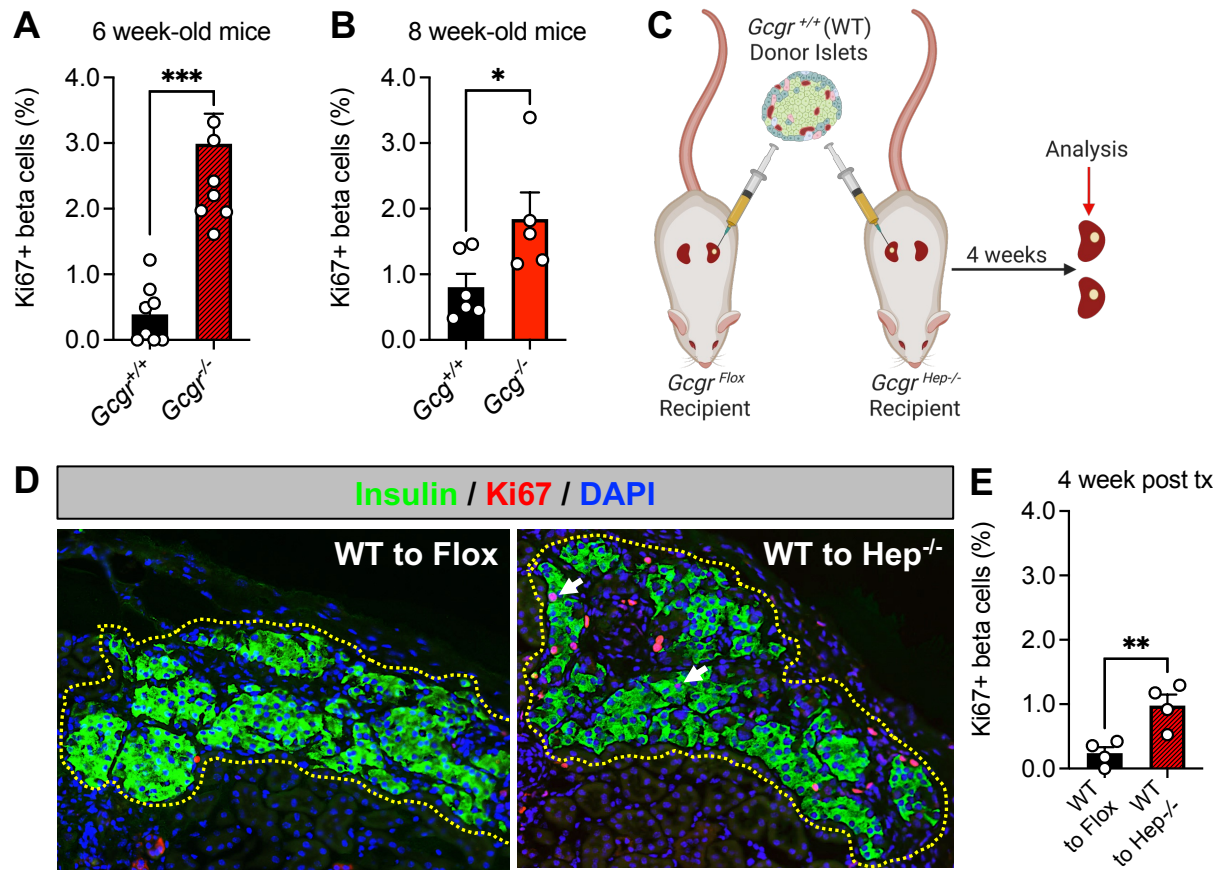


**Figure 3**



# Supplemental Figure 1



**Supp Fig 2: Slc7a2 is required for Gcgr-Ab-induced beta cell proliferation in transplanted mouse islets**

